EVALUATION OF THREE-DIMENSIONAL J-INTEGRAL OF SEMI-ELLIPTICAL SURFACE CRACK IN PRESSURE VESSEL

M. KIKUCHI, H. MIYAMOTO
Science University of Tokyo,
Department of Mechanical Engineering, Noda City, Chiba 278, Japan

Y. SAKAGUCHI
Kure Works, Babcock-Hitachi K.K.,
Kure Works, No. 6-9 Takara-Machi, Kure-Shi, Hiroshima-Ken 737, Japan

Summary.

J integral is expected to be one of the criterion of fracture in elasto-plastic state. Rice showed firstly the equation of J integral in two dimensional expression. Many experimental and analytical studies have been carried out by using this expression. But when a semi-elliptical surface crack in pressure vessel is considered, it is necessary to extend the equation to three dimensional expression. It is convenient to use Eshelby's energy momentum tensors to carry out this extension. By using energy momentum tensors, it is shown that J integral is the force acting on elastic singularities (including crack tips), or elastic inhomegeneities. Then, J integral is the force vector having three components J_x, J_y and J_z, and the direction of the vector can be determined. The direction of the vector may be related to the direction of the crack extension.

In this paper, expressions of J_x, J_y and J_z are introduced, and the evaluation of these values are carried out by using finite element analysis.

Firstly, the through crack problem in a thick plate is analysed. J_x values are evaluated at several points along the crack front. Two dimensional analyses are also carried out for plane stress and plane strain states. It is shown that the J_x values of inner part of plate coincide with the results of plane strain state analysis, and near free surface region, J_x value agrees with the result of plane stress state analysis. Especially at the free surface, J_x value becomes small.

Secondly, the semi-elliptical surface crack problem is analysed. J_x and J_y values are evaluated and compared with the penny shape crack problem. The magnitude and the direction of the force vector J_x and J_y are determined by next equations.

$$\bar{J} = \sqrt{J_x^2 + J_y^2}\,, \qquad \theta = \arctan(J_y/J_x).$$

It is shown that $\bar{J}$ and θ values of the deepest part of the crack agree with the results of penny shape crack problem, and near free surface region, the discrepancies between these values become large.

Thirdly, the semi-elliptical surface crack problem in pressure vessel is analysed. To evaluate the effects of pressure acting on crack surfaces, an additional term to J integral expression is introduced. For this problem, by using r-θ-z coordinate is used, then J_r and J_z values are evaluated. Several cases for different crack shapes and load conditions are analysed and the effects of crack shapes on crack extension are discussed.

1. Expressions of three components of J vector.

Eshelby[1] has shown the J integral expression as the force acting on crack tips by next equations.

$$F_\ell = \int_\Gamma P_{j\ell} dS_j \tag{1}$$

$$P_{j\ell} = W\delta_{j\ell} - \sigma_{ij} u_{i,\ell} \tag{2}$$

where ℓ is the direction of force vector, Γ denotes the arbitrary surface surrounding the crack and $P_{j\ell}$ is called energy momentum tensor. Eq.(1) and (2) can be applied to three dimensional crack problem as follows.

Consider the section of three dimensional crack front as in Fig.1. The crack front coincides with z axis, and the closed surface surrounding the crack front is composed of S1-S2-S3. When ℓ=x, eq.(1) becomes to

$$F_x = \int_{S1+S2+S3} P_{jx} dS_j = F_x^1 + F_x^2 + F_x^3. \tag{3}$$

where
$$F_x^1 = B\int_\Gamma (W dy - \sigma_{ij} n_j u_{i,x} ds_j), \tag{4}$$

$$F_x^2 = -\int_{S2} \sigma_{iz} u_{i,x} ds , \tag{5}$$

$$F_x^3 = \int_{S3} \sigma_{iz} u_{i,x} ds . \tag{6}$$

As F_x depends on the width B in Fig.1, so J_x value at point o is obtained by next equation.

$$J_x = \lim_{B\to o} \frac{1}{B} F_x = \int_\Gamma (W dy - \sigma_{ij} n_j u_{i,x} ds_j) - \int_S (\sigma_{iz} u_{i,x})_{,z} dS. \tag{7}$$

In the case of two dimensional problem, σ_{iz} becomes zero (for plane strain state, σ_{zz} is not zero but constant and the differential by z becomes zero) and eq.(7) coincides with the one shown by Rice[2].

It can be considered when ℓ=y or z by the same procedure and results are expressed as;

$$J_y = \int_\Gamma (-W dy - \sigma_{ij} n_j u_{i,y} ds_j) - \int_S (\sigma_{iz} u_{i,y})_{,z} dS, \tag{8}$$

$$J_z = -\int_S (\sigma_{iz} u_{i,z})_{,z} dS. \tag{9}$$

These values J_x, J_y and J_z are the three components of J vector and each of these values means the force acting on the crack front along x, y and z axis. When a symmetrical two dimensional crack is considered, it is enough to evaluate only J_x value, but for three dimensional case, it is necessary to consider other two components of J vector.

Moreover, if the crack surfaces are pressurized, an additional term has to be considered as

$$J_{\ell ad.} = -\int_{\Gamma'} (\sigma_{ij} n_j u_{i,\ell}) ds_j. \tag{10}$$

where Γ' means the crack surface. When crack surfaces are unpressurized, σ_{ij} is zero on Γ'

and eq.(10) becomes zero.

2. J_x values of the through crack in a thick plate.

Fig.2 shows the through crack in a thick plate. Sih et al.[3] and Benthum[4] have studied the surface crack problems analytically, and obtained the results that the stress singularity vary near free surface region. In this section, the same problem is analysed and J_x values are evaluated.

Fig.3 shows the mesh division and the dimensions in x-y plane. To evaluate J_x values, the path integral method is employed and three pathes used are also shown in Fig.3. Fig.4 shows the mesh division in x-z plane. As it is considered that stresses and strains vary abruptly near free surface, the plate is divided into seven layers by two types of division. Fig.4(a) shows that mesh is divided equally along z axis and (b) shows that the mesh is divided finely near free surface and coarsely in the center of the plate.

The results obtained are shown in Fig.5. By using finite element method, J_x is evaluated as F_x/B, where B is the width of the mesh division along z axis. In Fig.5, it is shown that J_x values become smaller at the free surface layer. As the free surface is in plane stress state, so J_x values are considered to be the maximum. But by this analysis, J_x values become the maximum in the second layer.

To examine this results, two dimensional analyses are carried out by using the same mesh as in Fig.3 for both plane stress and plane strain states. The results are shown in Table I with the results of unequally divided case. It is noticed that at the center of the plate, J_x values agree well with the results of plane strain analysis, and at the second layer they agree with the results of plane stress analysis. These phenomena cause the diminution of σ_z at the free surface and may be related to Sih's results that K_1 value becomes suddenly small at the free surface.

3. J_x and J_y values of semi-circular surface crack.

When a semi-circular surface crack is considered, as shown in Fig.6, both J_x and J_y values must be evaluated. The magnitude and the direction of J vector are determined by next equations.

$$\overline{J} = \sqrt{J_x^2 + J_y^2}\ , \tag{11}$$

$$\theta = \arctan(J_y/J_x). \tag{12}$$

Fig.7 shows the $\overline{J}$ values obtained by this analysis. Two types of mesh division are also used in this analysis. $\overline{J}$ values become the maximum at the free surface and become the minimum at the bottom of the crack. At the bottom of the crack, $\overline{J}$ value, the average of three pathes, is 1.644×10^{-3} kgf/mm and the theoretical value of the penny shape crack is 1.655×10^{-3} kgf/mm. The agreement of them is very good.

The directions of the J vectors are shown in Fig.8 for unequally divided case. Results are shown as the average value of three pathes. At the bottom of the crack, the directions of J vector coincide with the radial axis from the center of the crack, but near free surface the vector tends to the inner side of the plate.

4. J vectors of the semi-elliptical surface crack in a pressure vessel.

Fig.9 shows the semi-elliptical surface crack in a pressure vessel. The crack exists on

the inner surface of the vessel. Finite element analyses are carried out by using the cylindrical coordinate and it is easy to rewrite eq.(7)-(10) by using this coordinate system. Fig. 10 shows the dimensions and coordinate of the pressure vessel. J vectors are evaluated at the seven segments along the crack front as shown in Fig.11. The pressure p acting on the inner surface of the vessel is assumed to be p=1.0 kgf/mm^2.

Four types of crack shapes are used by changing a value as a/c=0.33, 0.5, 0.7 and 0.9. The crack of a/c=0.33 is the recommended shape by ASME. For each shape of crack, two analyses are carried out, one is that the crack surfaces are pressurized and the other is unpressurized. All of these analyses are carried out in elastic states. Three pathes are used for evaluation of J vectors and the results are shown as the average values of the three pathes.

The results are shown in Fig.12-15 and Table II-V.

Fig.12-14 and Table II-III show the J_r, J_z and $\overline{J}$ values. It is noticed that as a/c becomes large, $\overline{J}$ values become large. Although it is reasonable that large crack depth results in large $\overline{J}$ values, it is interesting to notice that J_z values increase rapidly at the inner surface of the vessel and J_r values increase slowly at the bottom of the crack. As the results, $\overline{J}$ values increase rapidly at the inner surface as increasing a/c value. The maximum point of $\overline{J}$ is the bottom of the crack for small a/c values, but when a/c=0.9, the inner surface of the vessel becomes the maximum point. And the minimum point of $\overline{J}$ moves from the inner surface to the bottom of the crack as increasing a/c values. It is the third segment when a/c=0.7 and the fifth segment when a/c=0.9.

These results mean that

i) when a/c values are small, the crack tends to extend along r axis, and

ii) when a/c values become large, the crack tends to extend along z axis.

Especially it is interesting that when a/c increases from 0.7 to 0.9, J_z value at the inner surface becomes larger than J_r values at the bottom of the crack, and $\overline{J}$ values also change with the same tendencies. These facts results that the semi-elliptical surface crack in pressure vessel extends keeping a/c$\fallingdotseq$0.8, if J_{IC} is constant along crack front. This result agrees well with the experimental results[5] that surface crack extends keeping a/c=0.8.

Fig.15 shows the directions of J vector for crack surface is unpressurized case. Corresponding to the results mentioned above, the directions of J vector change little at the bottom of the crack, but at the inner surface they turn to z axis as a/c increases.

Table IV shows the effect of the pressure acting on crack surfaces. For all a/c values, $\overline{J}$ increases about 10-14% by considering the pressure on crack surfaces, and they increase a little as increasing a/c values. By this results, it means that K_1 values increase 5-7% by the pressure on crack surfaces.

A.S.Kobayashi[6] obtained K_1 value at the bottom of the surface crack in pressurized cylinder where crack surfaces are unpressurized. To compare with his results, K_1 values are calculated by using $\overline{J}$ values at the bottom of the crack by next equation.

$$K_1 = \sqrt{\overline{J}E/(1-\nu^2)}. \qquad (13)$$

The results are shown in Table V. The differences of the two values is 4.2% when a/c=0.33 and it becomes small as a/c increases.

5. Conclusions.

The results are suumerized as follows.

1) It is pointed out that J integral is the force vector acting on crack tips and the expressions of three components of J vector are introduced by using energy momentum tensors.

2) A through crack and a part through crack problems are analysed and J vectors are obtained. Especially, the diminution of J_x values at the free surface are observed for through crack problem.

3) Semi-elliptical surface crack problems in a pressure vessel are analysed for 4 types of crack shape. The results show that

a) crack extends keeping a/c≈0.8,

b) $\bar{J}$ values increase about 10-14% by considering the pressure acting on crack surfaces,

c) K_1 values calculated by these analyses agree well with the results obtained by A.S. Kobayashi.

Acknowledgement.

Authors wish to express their appreciations to Mr. H. Uematsu and Mr. I. Yamamoto, students of Science University of Tokyo, for their supports and helpful discussions.

References

[1] Eshelby, J.D., Solid State Physics, Eds. by F.Seitz and D.Turnbull,pp.79(1956)

[2] Rice, J.R., Fracture 2, Ed. by Liebowitz. PP.191(1968)

[3] Sih, G.C. and Hartranft, R.J., Int. Journ. of Fracture, Vol.9, No.1, pp.75(1973)

[4] Benthum, J.P., Report No.663, Laboratory of Engineering Mechanics, (Delft Univ. of Technology, 1975)

[5] Takano,T., and Okamura,H., 2nd Symposium of HPI,pp.94(1978)

[6] Kobayashi, A.S., Proc. of the Japan-U.S. Seminor, Eds. by Kanazawa, T. and Kobayashi, A.S., pp.127(1973)

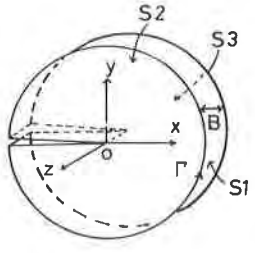

Fig.1 The section of three dimensional crack.

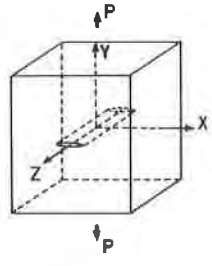

Fig.2 The through crack in a thick plate.

Tables.

Table I. J_x values of the through crack with J values of two dimensional cracks.

No. of path. / No. of layer.	Unequally divided case.		
	1	2	3
1	6.24	6.16	5.64
2	6.48	6.28	6.00
3	6.36	6.24	5.96
4	6.26	6.10	5.82
5	6.10	5.94	5.68
6	5.94	5.78	5.54
7	5.82	5.70	5.46
Plane stress.	6.46	6.22	6.00
Plane strain.	5.78	5.62	5.40

($\times 10^{-3}$ kgf/mm)

Talbe II. J_r and J_z values when crack surfaces are unpressurized. (kgf/mm)

No. of segment	a/c = 0.33		a/c = 0.5		a/c = 0.7		a/c = 0.9	
	J_r	J_z	J_r	J_z	J_r	J_z	J_r	J_z
1	0.345	0.791	0.272	1.508	0.252	2.699	0.248	3.676
2	0.844	0.683	0.838	1.471	0.783	2.499	0.740	3.539
3	1.155	0.563	1.326	1.223	1.346	2.135	1.302	3.032
4	1.461	0.458	1.792	0.965	1.925	1.685	1.968	1.527
5	1.749	0.326	2.203	0.657	2.457	1.126	2.531	1.527
6	1.940	0.123	2.517	0.241	2.873	0.405	2.961	0.561

Table III. J_r and J_z values when crack surfaces are pressurized. (kgf/mm)

No. of segment	a/c = 0.33		a/c = 0.5		a/c = 0.7		a/c = 0.9	
	J_r	J_z	J_r	J_z	J_r	J_z	J_r	J_z
1	0.391	0.882	0.311	1.680	0.295	2.893	0.295	4.161
2	0.937	0.759	0.932	1.635	0.883	2.807	0.843	4.003
3	1.277	0.623	1.471	1.358	1.513	2.397	1.475	3.426
4	1.617	0.507	1.989	1.072	2.163	1.893	2.225	2.633
5	1.939	0.362	2.445	0.731	2.762	1.267	2.866	1.731
6	2.149	0.136	2.793	0.265	3.233	0.456	3.360	0.635

Table IV. Incremental ratios of $\overline{J}$ by considering the pressure on crack surfaces.

$$\frac{(\overline{J}_{pr.} - \overline{J}_{unpr.})}{\overline{J}_{unpr.}} \times 100.$$

No. of layer.	a/c			
	0.33	0.5	0.7	0.9
1	10.8	10.9	12.5	13.4
2	10.8	11.0	12.4	13.3
3	10.7	11.0	13.1	13.0
4	10.7	11.0	12.3	13.0
5	11.0	11.2	12.4	13.1
6	11.7	11.5	12.6	13.2

Table V. Comparison of K_1 values with the results by A.S.Kobayashi.

a/c	0.33	0.5	0.7	0.9
K_1 by A.S.Kobayashi	221.2	236.4	253.7	264.3
$K_1=\sqrt{\overline{J}E/(1-\nu^2)}$	211.8	241.6	258.5	263.6
Difference(%)	4.2	2.2	2.0	0.3

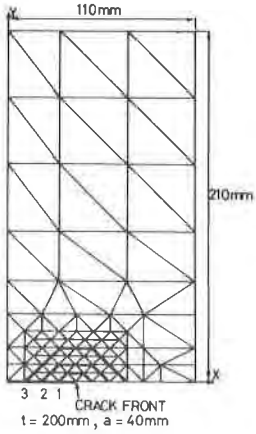

Fig.3 Mesh division of the thick plate in x-y plane.

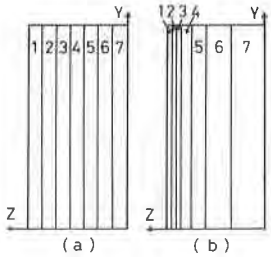

Fig.4 Mesh division of the thick plate in y-z plane.
(a) Equally divided,
(b) Unequally divided.

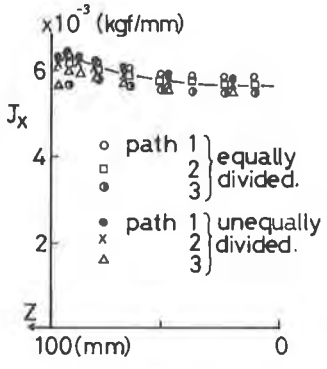

Fig.5 J_x values of the through crack problem.

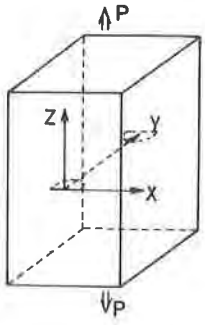

Fig.6 The semi-circular surface crack in a thick plate.

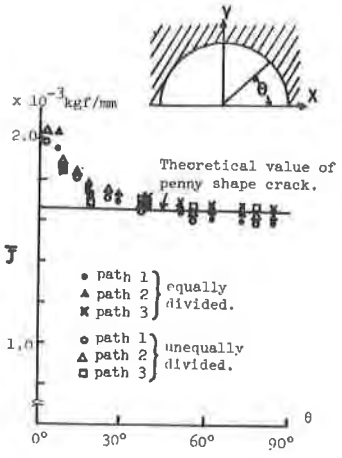

Fig.7 $\bar{J}$ values of the semi-circular surface crack.

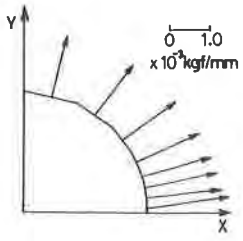

Fig.8 Directions of J vectors of the semi-circular surface crack. (Unequally divided.)

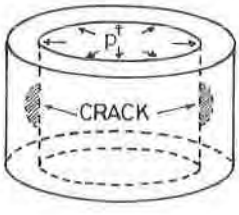

Fig.9 The semi-elliptical surface crack in a pressure vessel.

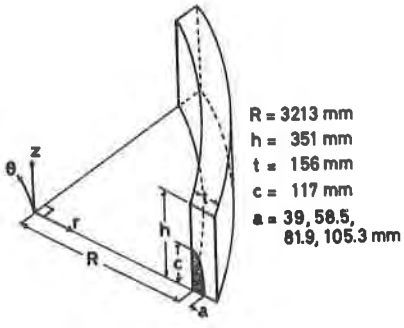

Fig.10 Dimensions and coordinates for the analyses.

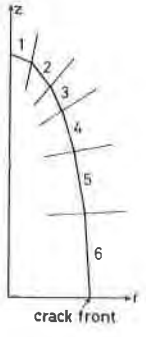

Fig.11 Seven segments of the crack front to evaluate J vectors.

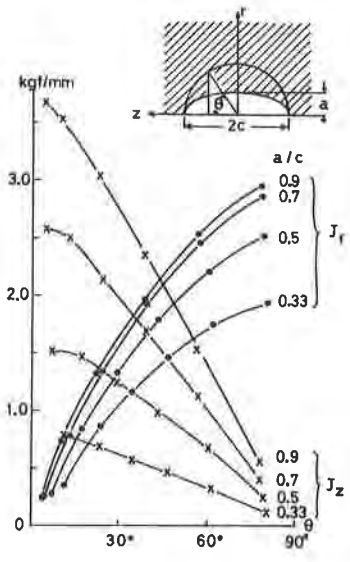

Fig.12 J_r and J_z values when crack surfaces are unpressurized.

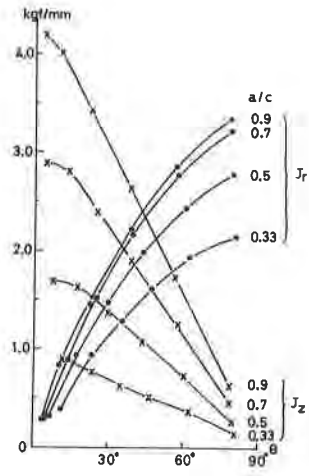

Fig.13 J_r and J_z values when crack surfaces are pressurized.

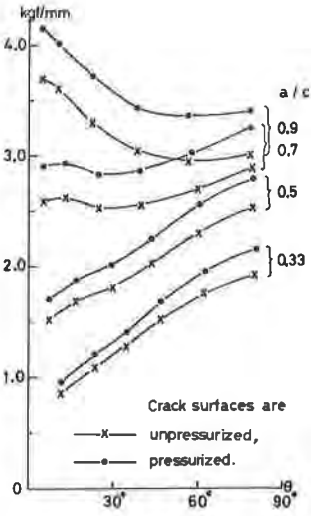

Fig.14 $\bar{J}$ values for each crack shape and load condition.

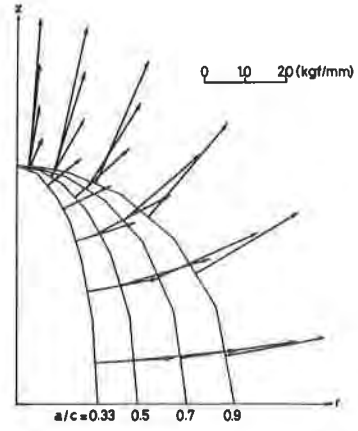

Fig.15 J vectors for four crack shapes. (Unpressurized.)